Mater Renew Sustain Energy (2016) 5:19
DOI 10.1007/s40243-016-0082-0

BRIEF COMMUNICATION

CO_2 electroreduction on P4VP modified copper deposited gas diffusion layer electrode: pH effect

Niyazi Alper Tapan[1]

Received: 22 July 2016 / Accepted: 20 September 2016 / Published online: 13 October 2016

Abstract Copper-based electrodes have high potential to convert CO_2 to valuable chemicals with satisfactory faradaic efficiency and selectivity. To improve these criteria, we have utilized the idea of copper deposited gas diffusion electrode and pH sensitive polymer membrane, poly(4-vinylpyridine) (P4VP). At pH 3.87, in contrast to pH 6.7, both faradaic efficiency and formic acid concentration increased after P4VP loading. Distinct behavior of P4VP at pH 3.87 indicates that P4VP could actively participate in formic acid production route by decoupled proton–electron transfer.

Keywords Poly(4-vinylpyridine) · CO_2 · Electroreduction, pH

Introduction

To mitigate the effects of CO_2 contribution to global warming, research works focus on conversion of low concentration (3-10 %) CO_2 into hydrocarbons, formic acid or alcohols by electrocatalytic routes. Research efforts based on copper, copper alloy or copper oxides have shown that these electrodes have high potential to convert CO_2 into CO, methane, ethylene, formic acid or alcohols with high faradaic efficiency and selectivity [1–18]. In addition, cathode electrode design was also studied by application of carbon-based gas diffusion layer (GDL) to decrease CO_2 mass transport resistance during CO_2 electroreduction [19–21]. With the deposition of metal or metal alloys on GDL, it is possible to work at high current densities because of nanospace, high pressure and hydrophobic environment created in the carbon fiber matrix structure. It was seen that although faradaic efficiency and selectivity of reduction products do not differ significantly, partial current densities on GDL supported electrodes are higher than bulk electrodes and are comparable to performances at high pressures [19, 22]. Of course, the increase in electrochemical performance is not only due to nanospace environment but also due to advanced microstructure of GDL [23].

In addition to the idea of GDL, incorporation of gas separation membranes like poly(4-vinylpyridine) (P4VP) opens new perspectives to increase the activity and selectivity of CO_2 electroreduction catalyst. It is known that active ligands such as pyridine in metal coordinated hydrophobic P4VP polymer membrane act as electron donation centers for CO_2 electroreduction both in non-aqueous and aqueous solvents or, by transforming in different pH media, these ligands attack oxygen atom of CO_2 [24, 25].

In many previous works [25–28], although researchers are well aware of the hydrophobicity of P4VP polymer membrane, it is very well known that the selectivity of P4VP was linked to the active ligands such as pyridine that act as electron donation centers for CO_2 electroreduction both in aqueous solvents or transformation of P4VP polymer in different pH media leading these ligands attack oxygen atom of CO_2. It is also very well known that other than hydrophobicity of P4VP, the CO_2 reduction mechanism is affected by the pH sensitivity of the polymer. If the pH of the electrolyte is less than the value of pKa of the P4VP, CO_2 adsorption onto P4VP layer occurs due to the acid base interaction between CO_2 and protonated pyridine

✉ Niyazi Alper Tapan
atapan@gazi.edu.tr

[1] Department of Chemical Engineering, Gazi University, Maltepe, 06570 Ankara, Turkey

residue. Even in weak acidic electrolytes where P4VP is partially protonated, this proton exchange on pyridine occurs sufficiently. Therefore, apparently, CO_2 concentration increases by adsorption onto P4VP, and higher concentration of CO_2 in the proximity of the catalysts can favor the reduction of CO_2 [25].

In this study, we have decided to combine the advantages of microstructure and pH sensitivity of GDL and P4VP for CO_2 electroreduction. We have investigated the effect of P4VP loading on the CO_2 electroreduction of copper deposited GDL in different pH environments.

Materials and methods

GDL disk deposited with Cu were used as working electrodes. A disk electrode of TGH-120 Toray carbon paper [Fuel Cell Store Inc. (336 μm thickness)] with a geometric surface area of 0.1925 cm^2 was cut, and then Cu was electrodeposited onto GDL from a deposition bath at 0.5 °C charge.

GDL disk electrodes were connected to the titanium wire current collector by silver epoxy binder EPO-TEK® H20E (Epoxy Tech.). After binding GDL disk to the titanium wire, it was left in an otoclave at the minimum bond line cure schedule of 120 °C and 15 min. Electrodeposition of copper on GDL were carried out at room temperature and −0.5 V vs. Ag/AgCl in diluted baths (0.0088 M $CuSO_4$ + 0.0055 M H_2SO_4 + 1.42 M Na_2SO_4) under constant stirring speed of 200 rpm.

After deposition of copper on GDL (Cu/GDL), 0.82 mg/cm^2 of P4VP was dropcasted onto the electrodes. P4VP (MW. 60,000) powder was commercially available (Aldrich Chemical Co. Inc.) and used as 1 wt% in ethanol. Ethanol solvent was of commercially available at purest grade (Sigma Aldrich 99.8 % GC grade). After drop casting P4VP onto the electrode, ethanol solvent was evaporated at room temperature.

Electrochemical experiments were carried out in a three-electrode cell environment at room temperature. Electrochemical procedure is described in the previous studies [10]. All potentials were reported vs. the reversible hydrogen electrode (RHE).

Cyclic voltammetry (CV) experiments were performed at a scan rate of 1 or 50 mV s^{-1} by an Ivium A06075 potentiostat in a hanging meniscus mode. Chronoamperometric experiments were also performed with Ivium A06075 potentiostat at −1.1 and −0.65 V vs. RHE. Blank cyclic voltammograms were compared with the voltammograms performed in the same electrolytes purged with CO_2 (Linde 4.5) for 30 min until saturation. Buffer electrolytes (pH 3.87, 0.1974 M KH_2PO_4 + 0.0026 M H_3PO_4; pH 1.46, 0.1858 M H_3PO_4 +0.01402 M KH_2PO_4; pH 6.7, 0.1 M KH_2PO_4 + 0.1 M K_2HPO_4) used for electrochemical experiments were prepared from ultrapure water and high-purity reagents (Merck Suprapur, Sigma Aldrich TraceSelect).

Since the aim of this study was to investigate selective conversion of low CO_2 concentrations or atmospheric CO_2 on P4VP modified copper, and since CO_2 is sparingly soluble (∼0.039 mol/lt) in the phosphate electrolyte system as in water [29], phosphate electrolyte was decided to be the best choice.

Carbonate buffers instead of phosphate buffers could have been used for this study, but to eliminate the possibility of interference of direct carbonate reduction during CO_2 reduction, phosphate electrolyte was selected. From the previous studies, it was seen that the reduction peak observed at −0.6/−0.7 V vs. RHE in bicarbonate buffer and in phosphate buffer at pH 11.6 was due to the production of formate via direct bicarbonate reduction. Although carbonate reduction peak is observed in alkaline phosphate buffer (pH 11.6), this peak disappeared in near neutral (pH 6.7) or acidic phosphate buffer electrolytes (pH <6.7) [10, 30, 31]. This phenomenon was also seen on different electrode surfaces as well [32]. Therefore, our protic aqueous electrolyte solutions were prepared with near neutral or acidic phosphate buffers.

All current densities are based on the electrochemical surface areas of electrodes. Electrochemical surface areas of electrodes were determined by multiplication of relative roughness with the geometrical surface area (the surface roughness factor of disk polycrystalline Cu which has a geometric surface area of 0.1925 cm^2 is used as the standard reference). The relative roughness of unmodified and P4VP modified copper deposited GDL was calculated by measuring their capacitance values in phosphate buffers at pH 6.7, 3.87, and 1.46 in a three-electrode electrochemical cell. Capacitance values were determined as described previously [33]. Capacitance values were normalized to the capacitance of polycrystalline copper to obtain relative surface roughness factors and electrochemical surface areas.

Online electrochemical mass spectroscopy (OLEMS) and high-performance liquid chromatography (HPLC) were used to detect gas phase and liquid phase products during CO_2 reduction as described previously [27, 28, 34, 35].

Results and discussion

In Fig. 1a and b, it can be seen that the onset of hydrogen evolution reaction (HER) is earlier at pH 1.46 for both P4VP modified and unmodified copper deposited GDL. After P4VP loading, current densities dropped by almost

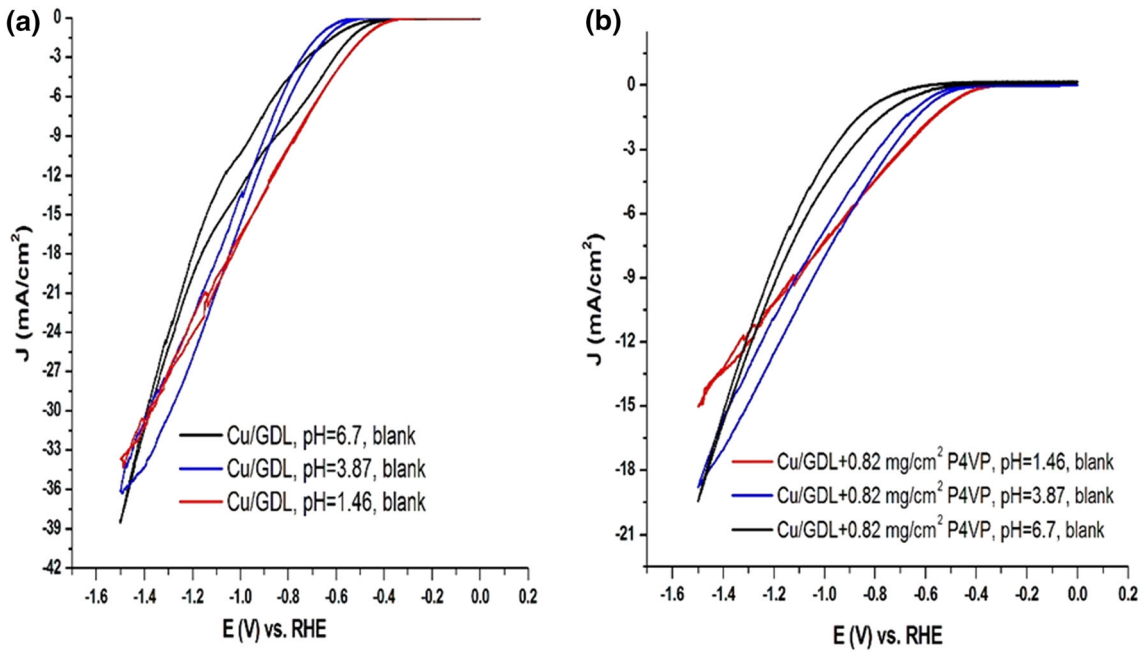

Fig. 1 CV curve of Cu/GDL with different P4VP loadings in phosphate buffer electrolyte at pH 1.46, 3.87, and 6.7. **a** Cu/GDL, blank electrolyte, and **b** Cu/GDL + 0.82 mg/cm^2 P4VP, blank electrolyte. Scan rate: 50 mV/s

half of unmodified electrodes, which indicates hydrogen suppression. As shown in Fig. 1, although reduction current densities dropped at pH 3.87 after P4VP loading, it was seen that the onset of HER shifted to less negative potentials. We believe that new buffer system formed by the encapsulation of P4VP on the electrode could provide lower HER overpotential than bare electrode surface at this pH level. At pH 6.7, after P4VP loading, the reduction currents dramatically dropped indicating that HER through proton reduction was greatly suppressed. HER suppression at pH 6.7 was also more significant compared to other pH levels on Cu/GDL. In this weak acidic electrolyte, since proton concentration is low, HER takes place through diffusion limited proton reduction [36] at early negative potentials and through water reduction at late negative potentials, and as the pH of the electrolyte increases, water reduction route dominates over proton reduction. This behavior is reflected by the increase of slope in voltammetry at late negative potentials close to ~ -1.1 V vs. RHE as reported before on cobalt protoporphyrin immobilized pyrolytic graphite [37]. After loading on Cu/GDL, P4VP may present as independent functional groups or encapsulate copper particles. In either position of P4VP, electrode system becomes dependent on the pH sensitivity or the ratio of protonation on P4VP. Earlier reports on modified graphite electrodes coated with P4VP/CoPc also show that the optimum condition of this protonic environment on P4VP was seen to be dependent on the pH of the electrolyte, since CO faradaic efficiency was maximized at a certain ratio of protonated to deprotonated pyridine groups in a pH condition close to the pKa of the polymer [25, 38].

Figure 2a shows that, after purging CO_2, two different reduction peaks were observed at ~ -0.7 and ~ -1.1 V vs. RHE at pH levels 6.7 and 3.87 on unmodified copper deposited GDL. In contrast to Fig. 2a, Fig. 2b shows that, all these peaks have disappeared after P4VP loading. The peak at ~ -0.7 V vs. RHE in Fig. 2a was previously observed on polycrystalline copper at pH 11.6 [10] and was ascribed to selective direct reduction of bicarbonate to formate. It was reported that the formation of bicarbonate is strongly affected by high local pH on copper nanoparticles or the buffer strength of the electrolyte. The origin of high local pH near copper nanoparticles is due to the release of OH^- during HER as the current density increases [7]. Therefore, we believe that high local pH and low buffer capacity could be favored in the proximity of copper nanoparticles on carbon fibers of GDL. The similarity of the position of the peak at -1.1 V vs. RHE with the previous reports of Hori et al. [39] in slightly acidic electrolyte indicate that it may be due to CO formation. Despite previous reports, the source of peak at -1.1 V vs. RHE could be different based on high or low buffer strength of the electrolyte. Since nanospace effect of fiber wall in the GDL increase local CO_2 partial pressure, it may help to increase the buffer strength and decrease pH close to pKa of buffer electrolyte. Therefore, nanospace effect may favor pH-dependent hydrocarbon formation route during CO_2 reduction either due to low pH or increase in local CO concentration and corresponding CO surface coverage [7]. It was

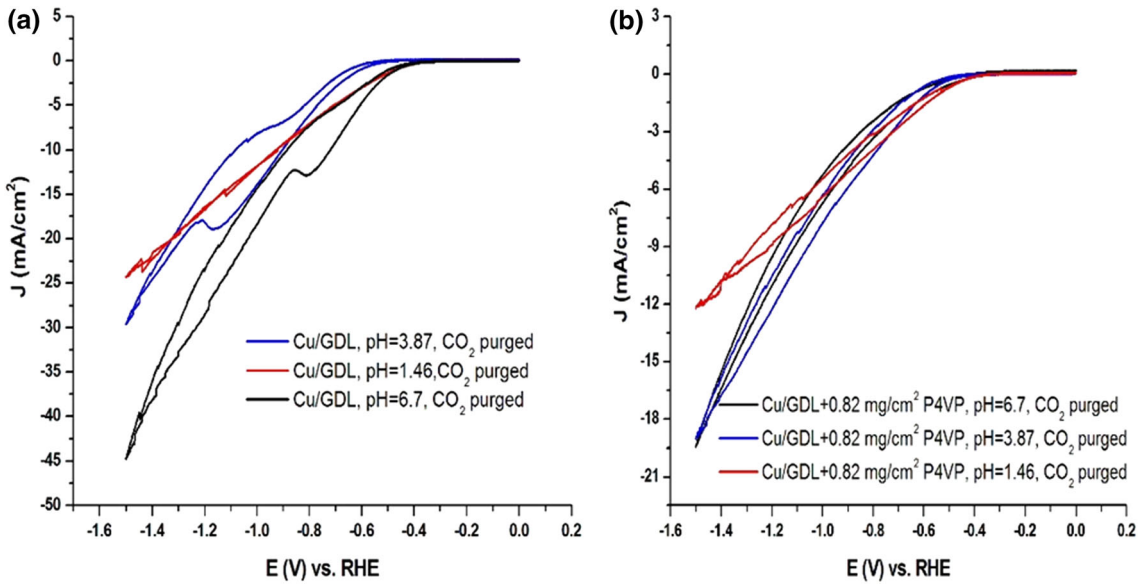

Fig. 2 CV curve of Cu/GDL with different P4VP loadings in phosphate buffer electrolyte at pH 1.46, 3.87 and 6.7. **a** Cu/GDL, CO_2-purged electrolyte, **b** Cu/GDL + 0.82 mg/cm^2 P4VP, CO_2-purged electrolyte. Scan rate: 50 mV/s

reported that even in slightly acidic electrolytes, CO formation increases dramatically and has higher selectivity compared to formate [40]. On the other hand, if the buffer strength is low, local alkalinity would lead to formation of bicarbonates and its direct reduction to formate.

Comparison of current densities of unmodified and P4VP modified Cu/GDL in both blank and CO_2-purged electrolytes also indicates that P4VP could induce mass transport resistance unlike when it is loaded on planar surfaces like copper foil [41]. We believe that this is due to the blocking effect of P4VP on the electrode surface other than the pH sensitivity. Whether or not there is HER on P4VP at low pH levels, if P4VP encapsulates copper particles, HER rate would be lower compared to unmodified copper particles on GDL.

CV experiments were also performed on both copper polycrystalline (model surface) and Cu/GDL in 1 M $KHCO_3$ (pH 6.7) to show the same type of behavior like in the case of phosphate buffer takes place after P4VP addition on copper polycrystalline and Cu/GDL in another media, and to show HER suppression effect and CO_2 reduction behavior (peaks) similar to Cu/GDL in phosphate buffer. As shown in Figs. 3 and 4, in 1 M $KHCO_3$, after P4VP loading, the reduction currents dropped for both copper polycrystalline and Cu/GDL like in the case of phosphate buffer indicating HER suppression. In this weak acidic electrolyte, the increase in the gap between two current profiles at late negative potentials show that water reduction was greatly suppressed by P4VP loading copper polycrystalline and Cu/GDL. As shown in Fig. 4, CV experiments with P4VP modified and unmodified copper polycrystalline and copper deposited GDL in CO_2-saturated 1 M $KHCO_3$ electrolyte also exhibit similar behavior like phosphate buffer. Although the same reduction peak at ~ -0.6 V vs. RHE was observed on copper polycrystalline and Cu/GDL in Figs. 3 and 4, after PVP loading, this peak was again completely diminished. Since the surface morphology of our electrode system differs too much from copper polycrystalline and since it is known that rough surfaces or under coordinated surface atoms caused by nanoparticle deposition may have different intrinsic activity, selectivity or local alkalinity [10, 42], the same experiments in 1 M $KHCO_3$ buffer were also repeated on Cu/GDL. As shown in Fig. 4b, higher reduction current densities were observed on unmodified Cu/GDL compared to copper polycrystalline, and in addition, the reduction peak at ~ -0.6 V vs. RHE was also more significant. On the other hand, after P4VP loading the reduction peak at -0.6 V vs. RHE diminished again similar to copper polycrystalline.

Figure 5 shows ion currents and current densities on Cu/GDL and P4VP modified Cu/GDL as a function of applied potential. The ion currents in Fig. 5c. indicate that the onset of HER was suppressed from $-0.7/-0.8$ to $-0.8/-0.9$ V vs. RHE for 0.82 mg/cm^2 P4VP loading and to ~ -1.2 V vs. RHE for 8.46 mg/cm^2 P4VP loading. The suppression of HER after P4VP loading could also be observed from the drop in current densities during CV.

Like hydrogen, the onset potentials of CH_4 shown in Fig. 5a also shifted to more negative potentials with P4VP loading. Although CH_4 formation started around $-0.7/-0.8$ V vs. RHE on unmodified electrode, after P4VP loading, it shifted to $-0.9/-1.0$ V vs. RHE at 0.82 mg/cm^2 loading and to $-1.1/-1.2$ V vs. RHE at 8.46 mg/cm^2

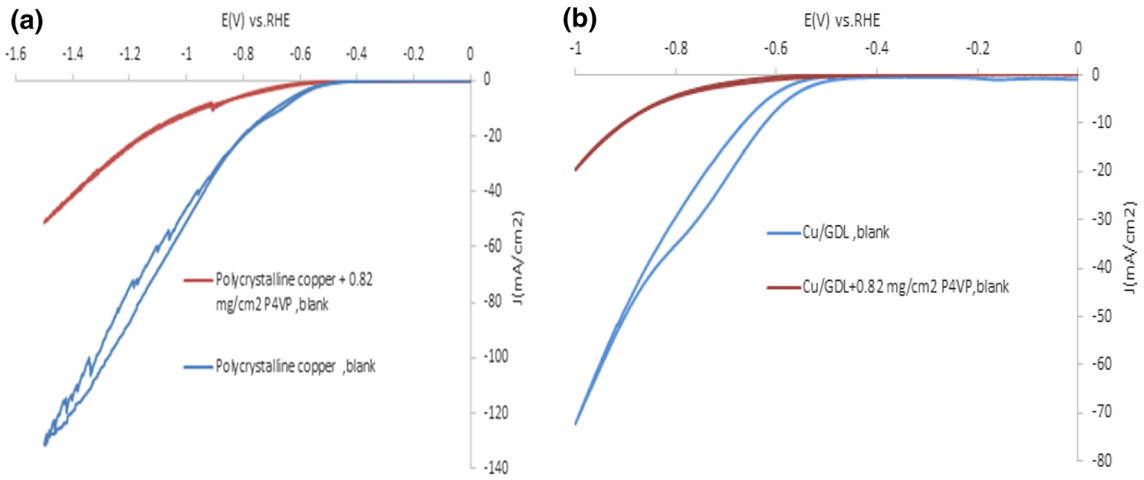

Fig. 3 CV curve of polycrystalline copper and Cu/GDL before and after P4VP loading in 1 M $KHCO_3$ electrolyte at pH 6.7. **a** Polycrystalline copper, blank electrolyte. **b** Cu/GDL, blank electrolyte. Scan rate: 50 mV/s

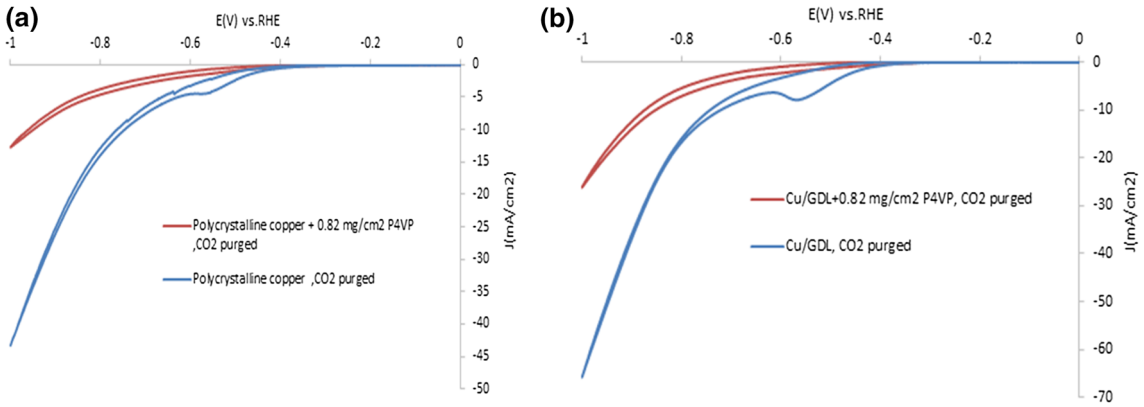

Fig. 4 CV curve of polycrystalline copper and Cu/GDL before and after P4VP loading in CO_2-purged 1 M $KHCO_3$ electrolyte at pH 6.7. **a** Polycrystalline copper, blank electrolyte. **b** Cu/GDL, blank electrolyte. Scan rate: 50 mV/s

loading. No onset potential shift could be observed during C_2H_4 formation; C_2H_4 formation started around −1.1 V vs. RHE on P4VP modified and unmodified electrodes. Close onsets of methane and ethylene fragments observed by OLEMS indicate proton–electron transfer mechanism for both ethylene and methane like on Cu (111) and copper polycrystalline [7, 43, 44]. Late onsets of CH_4 and C_2H_4 after P4VP loading indicate that CO_2 to CO pathway [44–48] forming hydrocarbons could be inhibited by P4VP loading on Cu/GDL.

Figure 6 shows offline HPLC results coupled with CV that were performed in different phosphate buffers at different pH levels. It was seen that onset of formic acid formation at pH 3.87 and 6.7 shifted to less negative potentials after P4VP loading. Early formic acid formation at these pH levels may be closely related with the change in the buffer strength of electrolyte on the electrode surface or proton stabilization or donation effect of P4VP [49] that encapsulates or neighbors copper catalyst centers. In fact, the results shown here are in agreement with high formic acid selectivity reported on P4VP modified copper foil electrode in 0.1 M $KHCO_3$ electrolyte (pH 6.8) [41]. At pH 1.46, no formic acid was detected. Although reduction currents dropped dramatically after P4VP loading, it was not reflected to formic acid production. As we have mentioned before, HER blocking effect of P4VP encapsulating copper particles plays a major role in the drop of reduction current densities. Although two reduced Py can evolve hydrogen, since the concentration of CO_2 in the saturated electrolyte is excessively greater than reduced pyridine, it was proposed that collision probability between PyH^0 and CO_2 is much higher than self interaction of two reduced Py to evolve hydrogen. In addition, it was also reported that since the calculated pKa values for PyH^0 are too high (pKa 27–31), it is not thermodynamically possible to create an environment for self quenching of PyH^0 [49]. At this point, we should also mention that the suppression effect of P4VP is seen both on hydrogen evolution and CO_2 reduction

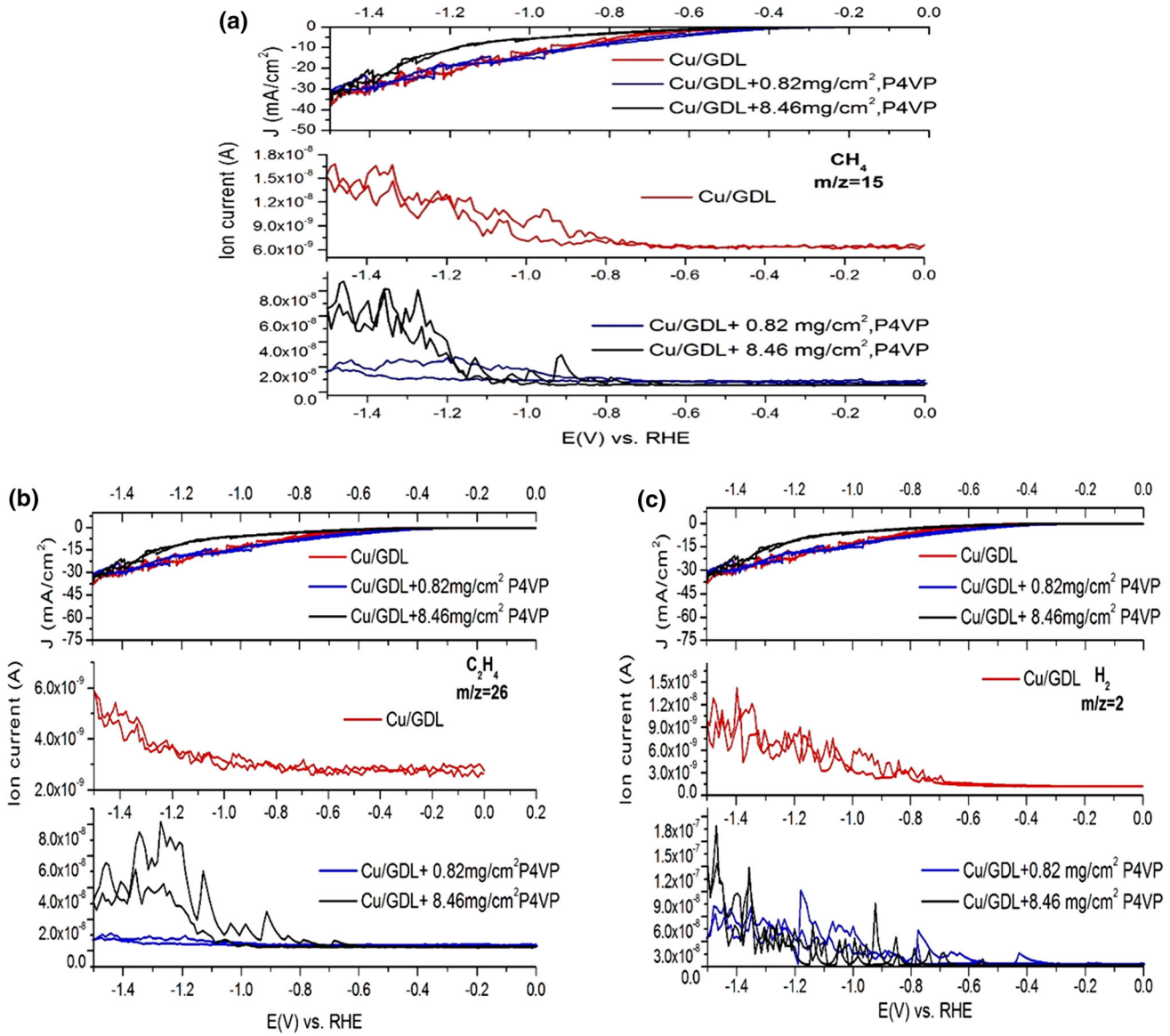

Fig. 5 Ion currents coupled with CV on unmodified and P4VP modified Cu/GDL as a function of applied potential in CO_2-saturated phosphate buffer electrolyte at pH 6.7 (scan rate 1 mV/s)

toward hydrocarbons. The drop in current densities after P4VP addition is a mixed effect of HER suppression and drop in hydrocarbon formation. And as it was mentioned in HPLC results above, although formic acid route is enhanced, it is not reflected on current densities, which means that hydrogen evolution and hydrocarbon formation are more dominant on current density–voltage behavior.

Like in the case of CO formation studied before [37, 50], the increase in formic acid production at higher pH levels mean that its production requires an intermediate like CO_2 anion which react with water. When P4VP is loaded on the electrode, if pH of the electrolyte is greater than pKa of P4VP (pKa 3.5), P4VP creates a less protonic environment by proton stabilization or activates CO_2 by forming metal bound CO_2 anion or $PyCO_2$ zwitter ionic complex [39, 49, 51].

Figure 7 shows the change in the faradaic efficiency of formic acid at pH 1.46, 3.87, and 6.7 for potentials −0.65 and −1.1 V vs. RHE during 2 h electrolysis. The rest of the faradaic efficiency shown in Fig. 7 is most probably shared by HER, CO, and hydrocarbon production. It was also seen in Fig. 7 that stable operation can be sustained in the potential range studied. At pH 1.46, faradaic efficiencies were extremely low; therefore, HER and hydrocarbon formation [52] could be dominant reactions at this pH level.

Figure 8 shows that, at pH 6.7, although formic acid concentration on P4VP modified electrode was lower than

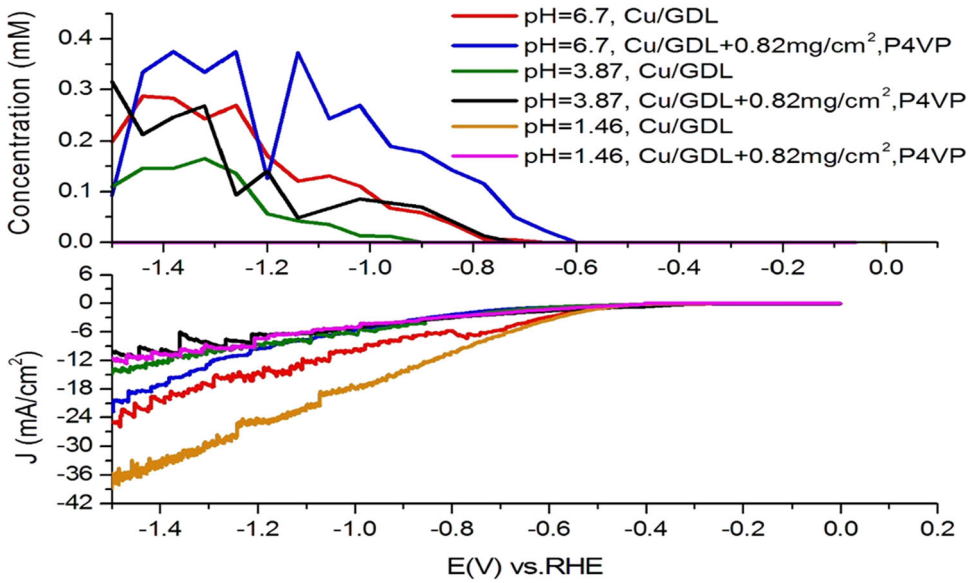

Fig. 6 Effect of electrolyte pH on voltammetric behavior and formic acid production activity of unmodified and P4VP modified Cu/GDL electrodes. Scan rate: 1 mV/s

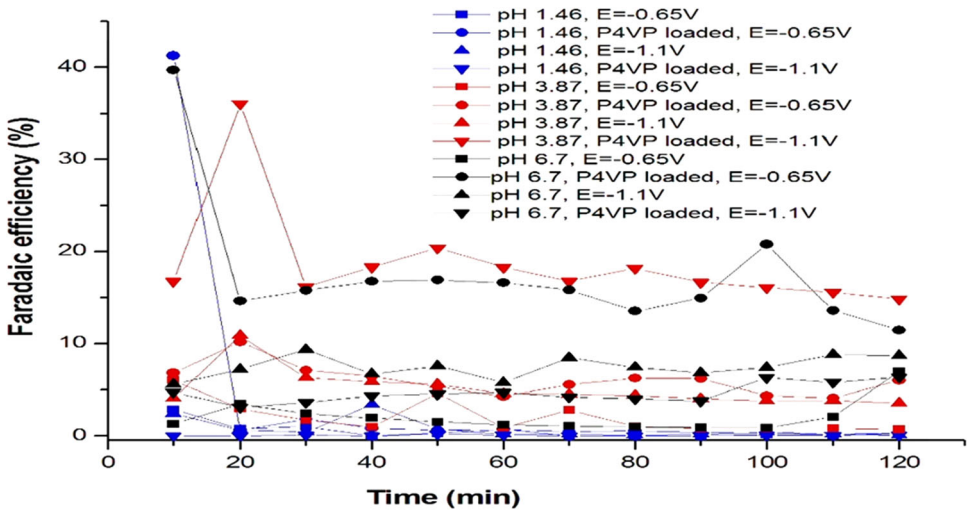

Fig. 7 Change of formic acid faradaic efficiency of P4VP modified and unmodified Cu/GDL with respect to time in different CO_2-purged phosphate buffers at different applied potentials

unmodified electrodeat −0.65 V vs. RHE, faradaic efficiency was higher. This situation clearly demonstrates HER suppression effect of P4VP. On the other hand, at −1.1 V vs. RHE, both formic acid concentration and faradaic efficiency were lower after P4VP modification. In Fig. 8, site blocking of P4VP can be clearly observed by looking at lower formic acid concentrations on P4VP modified electrodes compared to unmodified electrodes at the two applied potentials. An intriguing observation at −1.1 V vs. RHE on P4VP modified electrode was lower faradaic efficiency in contrast to higher formic acid concentration compared to −0.65 V vs. RHE. We believe that since water reduction cannot be blocked by P4VP, HER shares part of faradaic efficiency at −1.1 V vs. RHE. The behavior of unmodified electrodes at −1.1 V vs. RHE was different from P4VP modified electrodes: higher formic acid production and faradaic efficiency on unmodified electrode at −1.1 V vs. RHE compared to −0.65 V vs. RHE exhibit some similarity to the previous works on cobalt protoporphyrin; this similarity is in the sense of maximum CO faradaic efficiency at pH 3 in water reduction region (at −0.8 V vs. RHE). At this pH and potential, CO_2 anion reacts with water, and further reduction of CO is inhibited due to low proton concentration [30].

Figure 8 shows that both faradaic efficiency and formic acid concentration increased after P4VP loading at pH 3.87. This means that P4VP could actively participate in formic acid production route by decoupled proton electron transfer mechanism at this pH level [41]. Highest formic concentration (2.6 mM) and highest faradaic efficiency (15 %) was also attained at pH 3.87. Since the pH 3.87 is very close to the pKa of P4VP (3.5), it could be the optimum pH [25], above or below which the formic acid production could be proportional to the ratio of protonated

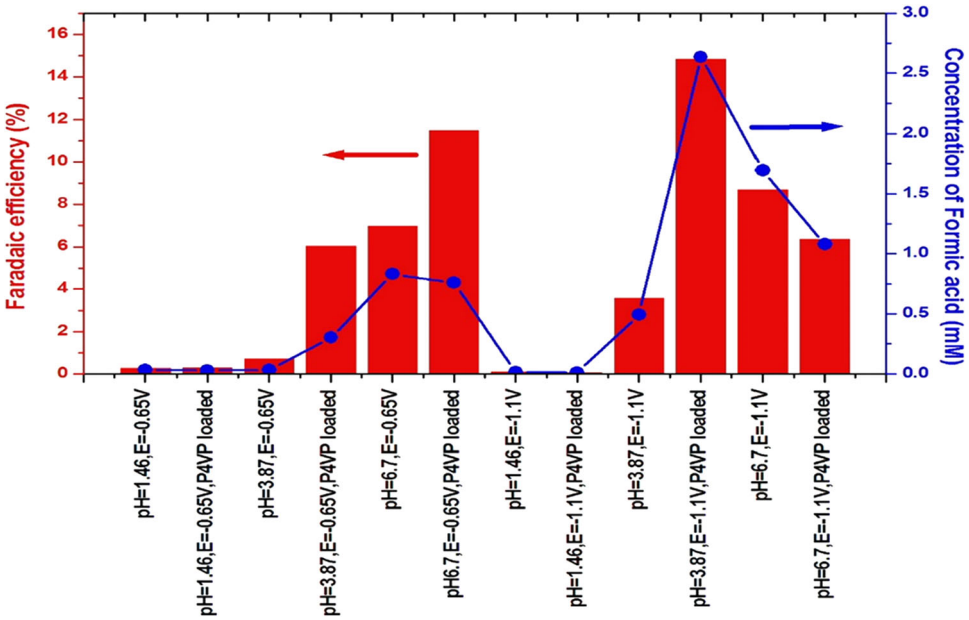

Fig. 8 Formic acid concentration and faradaic efficiency after 2 h of electrolysis on P4VP modified and unmodified copper deposited GDL in different CO_2-purged phosphate buffers at different applied potentials

to free pyridine species. At pH 3.87, it was also interesting to detect formic acid at low overpotential (0.65 V vs. RHE) and achieve significant faradaic efficiency, since HPLC results in Fig. 4 show almost no formic acid formation. This difference between HPLC-coupled voltammetry and HPLC-coupled electrolysis indicates that formic acid production is affected by the electrolysis time which maybe due to the possible copper dissolution and complexation with P4VP in the acidic environment [34].

Conclusions

In conclusion, the onset shifts at pH 6.7 and 3.87 by P4VP loading and higher faradaic efficiency and formic acid concentration on unmodified Cu/GDLat −1.1 V vs. RHE compared to −0.65 V vs. RHE could mean that the rate determining step is CO_2 activation to CO_2 anion on copper during formic acid production. Distinct behavior of P4VP modified Cu/GDL at pH 3.87 indicates that P4VP could actively participate in formic acid production route by decoupled proton–electron transfer mechanism.

Acknowledgments The author acknowledges the funding from TUBİTAK 2219 Post Doctoral Fellowship Programme and also would like to thank Leiden Institute of Chemistry faculty staff for their help during OLEMS and HPLC experiments.

References

1. Lim, R.J., Xie, M., Sk, M.A., Lee, J.-M., Fisher, A., Wang, X., Lim, K.H.: A review on the electrochemical reduction of CO_2 in fuel cells, metal electrodes and molecular catalysts. Catal. Today **233**, 169–180 (2014)
2. Katah, A., Uchida, H., Shibata, M., Watanabe, M.: Design of electrocatalyst for CO_2 reduction_ effect of the microcrystalline structures of Cu-Sn and Cu-Zn alloys on the electrocatalysis of CO_2 reduction. J. Electrochem. Soc. **141**, 2054–2058 (1994)
3. Watanabe, M., Shibata, M., Kato, A.: Design of electrocatalyst for CO_2 reduction III. The selective and reversible reduction of on Cu alloy electrodes. J. Electrochem. Soc. **138**, 3382–3389 (1991)
4. Rasul, S., Anjum, D.H., Jedidi, A., Minenkov, Y., Cavallo, L., Takanabe, K.: A highly selective copper-indium bimetallic electrocatalyst for the electrochemical reduction of aqueous CO_2 to CO. Angew. Chem. Int. Ed. Engl. **54**, 2146–2150 (2015)
5. Alvarez-Guerra, M., Quintanilla, S., Irabien, A.: Conversion of carbon dioxide into formate using a continuous electrochemical reduction process in a lead cathode. Chem. Eng. J. **207–208**, 278–284 (2012)
6. Kas, R., Kortlever, R., Milbrat, A., Koper, M.T., Mul, G., Baltrusaitis, J.: Electrochemical CO_2 reduction on Cu2O-derived copper nanoparticles: controlling the catalytic selectivity of hydrocarbons. Phys. Chem. Chem. Phys. **16**, 12194–12201 (2014)
7. Kas, R., Kortlever, R., Yılmaz, H., Koper, M.T.M., Mul, G.: Manipulating the hydrocarbon selectivity of copper nanoparticles in CO_2 electroreduction by process conditions. ChemElectroChem **2**, 354–358 (2015)
8. Keerthiga, G., Viswanathan, B., Chetty, R.: Electrochemical reduction of CO_2 on electrodeposited Cu electrodes crystalline phase sensitivity on selectivity. Catal. Today **245**, 68–73 (2015)
9. Kortlever, R., Balemans, C., Kwon, Y., Koper, M.T.M.: Electrochemical CO_2 reduction to formic acid on a Pd-based formic acid oxidation catalyst. Catal. Today **244**, 58–62 (2015)
10. Kortlever, R., Tan, K.H., Kwon, Y., Koper, M.T.M.: Electrochemical carbon dioxide and bicarbonate reduction on copper in weakly alkaline media. J. Solid State Electr. **17**, 1843–1849 (2013)

11. Le, M., Ren, M., Zhang, Z., Sprunger, P.T., Kurtz, R.L., Flake, J.C.: Electrochemical reduction of CO_2 to CH3OH at copper oxide surfaces. J. Electrochem. Soc. **158**, E45 (2011)
12. Galvita, V.V., Poelman, H., Detavernier, C., Marin, G.B.: Catalyst-assisted chemical looping for CO_2 conversion to CO. Appl. Catal. B: Environ. **164**, 184–191 (2015)
13. Peterson, A.A., Abild-Pedersen, F., Studt, F., Rossmeisl, J., Nørskov, J.K.: How copper catalyzes the electroreduction of carbon dioxide into hydrocarbon fuels. Energy Environ. Sci. **3**, 1311 (2010)
14. Qiao, J., Fan, M., Fu, Y., Bai, Z., Ma, C., Liu, Y., Zhou, X.-D.: Highly-active copper oxide/copper electrocatalysts induced from hierarchical copper oxide nanospheres for carbon dioxide reduction reaction. Electrochim. Acta **153**, 559–565 (2015)
15. Qiao, J., Jiang, P., Liu, J., Zhang, J.: Formation of Cu nanostructured electrode surfaces by an annealing–electroreduction procedure to achieve high-efficiency CO_2 electroreduction. Electrochem. Commun. **38**, 8–11 (2014)
16. Reske, R., Duca, M., Oezaslan, M., Schouten, K.J.P., Koper, M.T.M., Strasser, P.J.: Controlling catalytic selectivities during CO_2 electroreduction on thin Cu metal overlayers. J. Phys. Chem. Lett. **4**, 2410–2413 (2013)
17. Jia, F., Yu, X., Zhang, L.: Enhanced selectivity for the electrochemical reduction of CO_2 to alcohols in aqueous solution with nanostructured Cu–Au alloy as catalyst. J. Power Sources **252**, 85–89 (2014)
18. Alazmi, A.: CuZn Alloy—Based Electrocatalyst for CO2 Reduction. King Abdullah University of Science and Technology Thuwal, Kingdom of Saudi Arabia (2014)
19. Furuya, N., Yamazaki, T., Shibata, M.: High performance Ru-Pd catalysts for CO_2 reduction at gas-diffusion electrodes. J. Electroanal. Chem. **431**, 39–41 (1997)
20. Mahmood, M.N., Masheder, D., Harty, C.J.: Use of gas-diffusion electrodes for high-rate electrochemical reduction of carbon dioxide. Reduction at lead, indium- and tin-impregnated electrodes. J. Appl. Electrochem. **17**, 1159–1170 (1987)
21. Cook, R.L., MacDuff, R.C., Sammels, A.F.: High rate gas phase CO_2 reduction to ethylene and methane using gas diffusion electrodes. J. Electrochem. Soc. **137**, 607–608 (1990)
22. Yamamoto, T., Tryk, D.A., Hashimoto, K., Fujishima, A., Okawa, M.: Electrochemical reduction of CO2 in the micropores of activated carbon fibers. J. Electrochem. Soc. **147**, 3393–3400 (2000)
23. Mortazavi, M., Tajiri, K.: In-plane microstructure of gas diffusion layers with different properties for PEFC. J. Fuel Cell Sci. Technol. **11**, 021002 (2013)
24. Abe, T., Taguchi, F., Yoshida, T., Tokita, S., Schnurpfeil, G., Wöhrle, D., Kaneko, M.: Electrocatalytic CO_2 reduction by cobalt octabutoxyphthalocyanine coated on graphite electrode. J. Mol. Catal. A Chem. **112**, 55–61 (1996)
25. Abe, T., Yoshida, T., Tokita, S., Taguchi, F., Imaya, H., Kaneko, M.: Factors affecting selective electrocatalytic CO_2 reduction with cobalt phthalocyanine incorporated in a polyvinylpyridine membrane coated on a graphite electrode. J. Electroanal. Chem. **412**, 125–132 (1996)
26. Qiao, J.L., Liu, Y.Y., Hong, F., Zhang, J.J.: A review of catalysts for the electroreduction of carbon dioxide to produce low-carbon fuels. Chem. Soc. Rev. **43**, 631–675 (2014)
27. Costentin, C., Robert, M., Saveant, J.M.: Catalysis of the electrochemical reduction of carbon dioxide. Chem. Soc. Rev. **42**, 2423–2436 (2013)
28. Satoh, M., Yoda, E., Hayashi, T., Komiyama, J.: Potentiometric titration of poly(vinylpyridines) and hydrophobic interaction in the counterion binding. Macromol. **22**, 1808–18121 (1989)
29. Danckwerts, P.V.: Insights into chemical engineering: selected papers of P.V. Danckwerts. Elsevier, The Netherlands (1981)
30. Perez Sanchez, M., Souto, R.M., Barrera, M., Gonzalez, S., Salvarezza, R.C., Arvia, A.J.: A mechanistic approach to the electroformation of anodic layers on copper and their electroreduction in aqueous solutions containing $NaHCO_3$ and Na_2CO_3. Electrochim. Acta **38**, 703–715 (1993)
31. Smith, B.D., Irish, D.E.: A surface enhanced roman scattering study of the intermediate and poisoning species formed during the electrochemical reduction of CO2 on copper. J. Electrochem. Soc. **144**, 4288–4296 (1997)
32. Spichiger-Ulmann, M., Augustynski, J.: Remarkable enhancement of the rate of cathodic reduction of hydrocarbonate anions at palladium in the presence of caesium cations. Helv. Chim. Acta **69**, 632–634 (1986)
33. Li, C.W., Ciston, J., Kanan, M.W.: Electroreduction of carbon monoxide to liquid fuel on oxide-derived nanocrystalline copper. Nature **508**, 504–509 (2014)
34. Wonders, A.H., Housmans, T.H.M., Rosca, V., Koper, M.T.M.: On-line mass spectrometry system for measurements at single-crystal electrodes in hanging meniscus configuration. J. Appl. Electrochem. **36**, 1215–1221 (2006)
35. Kwon, Y., Koper, M.T.M.: Combining voltammetry with HPLC: application to electro-oxidation of glycerol. Anal. Chem. **82**, 5420–5424 (2010)
36. Strmcnik, D., Uchimura, M., Wang, C., Subbaraman, R., Danilovic, N., van der Vliet, D., et al.: Improving the hydrogen oxidation reaction rate by promotion of hydroxyl adsorption. Nat. Chem. **5**, 300–306 (2013)
37. Shen, J., Kortlever, R., Kas, R., Birdja, Y.Y., Diaz-Morales, O., Kwon, Y., et al.: Electrocatalytic reduction of carbon dioxide to carbon monoxide and methane at an immobilized cobalt protoporphrin. Nat. Commun. **6**, 8177 (2015)
38. Yoshida, T., Kamato, K., Tsukamoto, M., Iida, T., Schlettwein, D., Wöhrle, D., et al.: Selective electrocatalysis for CO_2 reduction in the aqueous phase using cobalt phthalocyanine/poly-4-vinylpyridine modified electrodes. J. Electroanal. Chem. **385**, 209–225 (1995)
39. Hori, Y., Murata, A., Takahashi, R.: Formation of hydrocarbons in the electrochemical reduction of carbon dioxide at a copper electrode in aqueous solution. J. Chem. Soc. Farad. T **1**(85), 2309–2326 (1989)
40. Sreekanth, N., Phani, K.L.: Selective reduction of CO_2 to formate through bicarbonate reduction on metal electrodes: new insights gained from SG/TC mode of SECM. Chem. Commun. **50**, 11143–11146 (2014)
41. Ponnurangam, S., Yun, C.M., Chernyshova, I.V.: Robust electroreduction of CO_2 at a poly(4-vinylpyridine)-copper electrode†. ChemElectroChem **3**(1), 74 (2015)
42. Tang, W., Peterson, A.A., Varela, A.S., Jovanov, Z.P., Bech, L., Durand, W.J., Dahl, S., Nørskov, J.K., Chorkendorff, I.: The importance of surface morphology in controlling the selectivity of polycrystalline copper for CO_2 electroreduction. Phys. Chem. Chem. Phys. **14**, 76–81 (2012)
43. Hori, Y.: Electrochemical CO_2 reduction on metal electrodes. In: Vayenas, C., White, R., Gamboa-Aldeco, M. (eds.) Modern Aspects of Electrochemistry, pp. 89–189. Springer, New York (2008)
44. Schouten, K.J.P., Qin, Z., Gallent, E.P., Koper, M.T.M.: Two pathways for the formation of ethylene in CO reduction on single-crystal copper electrodes. J. Am. Chem. Soc. **134**, 9864–9867 (2012)
45. Peterson, A.A., Norskov, J.K.: Activity descriptors for CO_2 electroreduction to methane on transition metal catalysts. J. Phys. Chem. Lett. **3**, 251–258 (2012)
46. Hatsukade, T., Kuhl, K.P., Cave, E.R., Abram, D.N., Jaramillo, T.F.: Insights into the electrocatalytic reduction of CO_2 on

metallic silver surfaces. Phys. Chem. Chem. Phys. **16**, 13814–13819 (2014)
47. Schouten, K.J.P., Kwon, Y., Van der Ham, C.J.M., Qin, Z., Koper, M.T.M.: A new mechanism for the selectivity to C1 and C2 species in the electrochemical reduction of carbon dioxide on copper electrodes. Chem. Sci. **2**, 1902–1909 (2011)
48. Calle-Vallejo, F., Koper, M.T.M.: Theoretical considerations on the electroreduction of CO to C2 species on Cu(100) electrodes. Angew. Chem. **125**, 7423–7426 (2013)
49. Lim, C.-H., Holder, A.M., Musgrave, C.B.: Mechanism of homogeneous reduction of CO_2 by pyridine: proton relay in aqueous solvent and aromatic stabilization. J. Am. Chem. Soc. **135**, 142–154 (2013)
50. Noda, H., Ikeda, S., Yamamoto, A., Einaga, H., Ito, K.: Kinetics of electrochemical reduction of carbon-dioxide on a gold electrode in phosphate buffer solutions. B. Chem. Soc. Jpn. **68**, 1889–1895 (1995)
51. Morris, A.J., McGibbon, R.T., Bocarsly, A.B.: Electrocatalytic Carbon dioxide activation: the rate-determining step of pyridinium-catalyzed CO_2 reduction. ChemSusChem. Energ. Mater. **4**, 191–196 (2011)
52. Schouten, K.J.P., Gallent, E.P., Koper, M.T.M.: The influence of pH on the reduction of CO and CO_2 to hydrocarbons on copper electrodes. J. Electroanal. Chem. **716**, 53–57 (2014)